TITLE PAGE

Large power increase enabled by high-Q diamond-loaded cavities for terahertz gyrotrons

Vitalii I. Shcherbinin[1,2] (0000-0002-9879-208X)
Konstantinos A. Avramidis[1] (0000-0001-9493-0468)
Ioannis Gr. Pagonakis[1] (0000-0003-3707-5391)
Manfred Thumm[1,3] (0000-0003-1909-3166)
John Jelonnek[1,3] (0000-0002-0531-7600)

[1]Institute for Pulsed Power and Microwave Technology, Karlsruhe Institute of Technology, 76131 Karlsruhe, Germany
[2]National Science Center "Kharkiv Institute of Physics and Technology", 61108 Kharkiv, Ukraine
[3]Institute of Radio Frequency Engineering and Electronics, Karlsruhe Institute of Technology, 76131 Karlsruhe, Germany

Abstract A new operation scheme is proposed to enable large increase in output power of terahertz gyrotrons. In this scheme, the gyrotron operates in weakly-attenuated dielectric modes supported by a conventional metal cavity, which is loaded with a coaxial rod made of ultralow-loss CVD diamond. Along with high ohmic Q-values, these modes are shown to possess rather strong beam-wave coupling, which ensures high interaction efficiency. As an example, the CVD diamond loading is applied to the cavity of the 527-GHz gyrotron developed at the Massachusetts Institute of Technology (MIT). The output power of this gyrotron operated in the high-Q dielectric mode is found to reach 140 W, compared to 15 W for the conventional-cavity tube. Using the coupled-mode approach, a new design is presented for a high-Q diamond-loaded cavity of the 527-GHz gyrotron. The designed cavity is shown to provide high-purity transformation of the operating dielectric mode to the outgoing mode of the hollow exit waveguide. The output mode can be extracted from the gyrotron using a standard output system and attains a peak power of 171 W, which is more than 11 times higher than that of the 527-GHz gyrotron with conventional cavity. The robustness of gyrotron performance against errors in manufacturing of the diamond-loaded cavity is discussed

Keywords gyrotron, ohmic losses, terahertz radiation, CVD diamond, output power

Declarations

Funding Partial financial support was received from the Alexander von Humboldt Foundation.

Conflicts of interest/Competing interests The authors declare no competing interest.

Ethics approval Not applicable

Consent to participate Not applicable

Consent for publication Not applicable

Availability of data and material Data are available from the authors upon reasonable request.

Code availability Not applicable

Authors' contributions All authors contributed to the study conception and design. Material preparation, data collection and analysis were performed by Vitalii I. Shcherbinin. The first draft of the manuscript was written by Vitalii I. Shcherbinin and all authors commented on previous versions of the manuscript. All authors read and approved the final manuscript.

Large power increase enabled by high-Q diamond-loaded cavities for terahertz gyrotrons

Vitalii I. Shcherbinin[1,2*], Konstantinos A. Avramidis[1], Ioannis Gr. Pagonakis[1], Manfred Thumm[1,3], and John Jelonnek[1,3]

[1]*Institute for Pulsed Power and Microwave Technology, Karlsruhe Institute of Technology, 76131 Karlsruhe, Germany*
[2]*National Science Center "Kharkiv Institute of Physics and Technology", 61108 Kharkiv, Ukraine*
[3]*Institute of Radio Frequency Engineering and Electronics, Karlsruhe Institute of Technology, 76131 Karlsruhe, Germany*

Abstract

A new operation scheme is proposed to enable large increase in output power of terahertz gyrotrons. In this scheme, the gyrotron operates in weakly-attenuated dielectric modes supported by a conventional metal cavity, which is loaded with a coaxial rod made of ultralow-loss CVD diamond. Along with high ohmic Q-values, these modes are shown to possess rather strong beam-wave coupling, which ensures high interaction efficiency. As an example, the CVD diamond loading is applied to the cavity of the 527-GHz gyrotron developed at the Massachusetts Institute of Technology (MIT). The output power of this gyrotron operated in the high-Q dielectric mode is found to reach 140 W, compared to 15 W for the conventional-cavity tube. Using the coupled-mode approach, a new design is presented for a high-Q diamond-loaded cavity of the 527-GHz gyrotron. The designed cavity is shown to provide high-purity transformation of the operating dielectric mode to the outgoing mode of the hollow exit waveguide. The output mode can be extracted from the gyrotron using a standard output system and attains a peak power of 171 W, which is more than 11 times higher than that of the 527-GHz gyrotron with conventional cavity. The robustness of gyrotron performance against errors in manufacturing of the diamond-loaded cavity is discussed.

Keywords gyrotron, ohmic losses, terahertz radiation, CVD diamond, output power

1. Introduction

In the sub-terahertz-to-terahertz range, second-harmonic gyrotrons are among the most powerful sources of continuous-wave radiation for a wide application in modern science and technology [1-4]. One of the major threats to operation of these gyrotrons is mode competition [5-15]. This threat comes mostly from the first-harmonic modes and generally increases with increasing gyrotron frequency. To avoid the mode competition, second-harmonic sub-terahertz gyrotrons are often designed to operate in the whispering-gallery modes [3, 6, 8, 9, 11, 15-17], which have reduced number of competing modes. Unfortunately, in metal gyrotron cavities, the whispering-gallery modes possess low ohmic quality factors Q_{ohm} and thus suffer from distinct power losses associated with cavity heating. The situation becomes particularly critical for second-harmonic gyrotrons with low beam power and broadband continuous frequency tuning [9, 15-19]. In these gyrotrons, long cavities are employed to provide continuous transition between high-order axial resonances of the operating mode. For conventional gyrotron cavities, the diffractive quality factor Q_{dif} scales as cube of the cavity length [19, 20]. Therefore, the increase of the cavity length lowers the ratio $P_{out}/P_{tot} = Q_{ohm}/(Q_{ohm} + Q_{dif})$ of the gyrotron output power P_{out} to the total wave power P_{tot} generated in the cavity. That is the reason why this ratio falls below 1/5 for present-day second-harmonic terahertz gyrotrons [16-18, 21], in which, as opposed to first-harmonic tubes [22], most of generated power is spent to heat the cavity walls. Moreover, ohmic losses in the gyrotron cavity weaken the strength of beam interaction with the operating mode and thereby reduce the beam-wave interaction efficiency (and P_{tot}) [23]. This loss-induced effect causes additional degradation of the gyrotron output power. As a result, for terahertz gyrotrons, high ohmic losses in the cavity can lower the output power P_{out} by a factor of more than 10 [23]. Up to now, these losses are considered to be unavoidable.

A possible way to overcome the constraint on output power can be provided by dielectric modes of a metal gyrotron cavity, which is loaded with a coaxial dielectric rod [13]. These modes can interact with conventional helical electron beams. More importantly, they possess high ohmic Q-values, provided that the loss tangent of the dielectric rod is small [13]. This property of dielectric modes makes them particularly attractive as operating modes for gyrotrons operated in the sub-terahertz-to-terahertz range. In this range, an ultralow-loss dielectric with exceptional material properties is the chemical vapor deposition (CVD) diamond [24-27]. The aim of this paper is to theoretically investigate the feasibility of terahertz gyrotrons, which are equipped with diamond-loaded cavities to operate in high-Q dielectric modes.

* vshch@ukr.net

2. High-Q modes of a metal cavity with coaxial diamond rod

Consider a mode of a cylindrical gyrotron cavity, which is made of metal and loaded with a coaxial dielectric rod. The radii of the cavity and coaxial insert are $R = R(z)$ and $R_i = R_i(z)$, respectively. The cavity mode has the angular frequency ω and the azimuthal index m. In cylindrical coordinates $\{r, \varphi, z\}$, the transverse fields of this mode can be expanded in terms of orthogonal normal (waveguide) modes as [28-32]

$$\mathbf{E}_\perp = \sum_n V_n(z)\mathbf{e}_{\perp n}(r) \qquad (1)$$
$$\mathbf{H}_\perp = \sum_n I_n(z)\mathbf{h}_{\perp n}(r)$$

$$\int_0^R r dr \langle \mathbf{e}_{\perp n}, \mathbf{h}_{\perp l} \rangle = \delta_{n,l} \qquad (2)$$

where $V_n(z)$ and $I_n(z)$ are the amplitudes of the transverse electric $\mathbf{e}_{\perp n}(r)$ and transverse magnetic $\mathbf{h}_{\perp n}(r)$ fields of the normal n-th mode, respectively, $\langle \mathbf{e}_{\perp n}, \mathbf{h}_{\perp l} \rangle = \left(e_{rn} h_{\varphi l} + e_{\varphi n} h_{rl}\right)$ is the inner product of $\mathbf{e}_{\perp n}(r)$ and $\mathbf{h}_{\perp l}(r)$ [33-35], $\delta_{n,l}$ is the Kronecker delta, and the field factor of the form $\exp(-i\omega t + im\varphi)$ is assumed, and omitted in the following. In what follows, cgs units are used unless otherwise stated.

For each normal mode, the transverse and longitudinal (axial) field components are related as

$$\mathbf{e}_\perp = \frac{i}{k_\perp^2}\left[k\left(\nabla_\perp h_z \times \mathbf{z}\right) + k_z \nabla_\perp e_z\right] \qquad (3)$$
$$\mathbf{h}_\perp = \frac{i}{k_\perp^2}\left[k_z \nabla_\perp h_z - \varepsilon k\left(\nabla_\perp e_z \times \mathbf{z}\right)\right]$$

where $\nabla_\perp = \hat{\mathbf{r}}\,\partial/\partial r + \hat{\boldsymbol{\varphi}}\, im/r$ is the transverse derivative operator, $k = \omega/c$, $k_z^2 = \varepsilon k^2 - k_\perp^2$, $\varepsilon = \varepsilon(r)$ is the relative permittivity of the cavity filling. The transverse wavenumber $k_\perp$ and the axial field components $h_z(r)$ and $e_z(r)$ are subject to Helmholtz equations, which are generally inhomogeneous and coupled equations for $\varepsilon = \varepsilon(r) \neq const$ [36].

In a hollow gyrotron cavity loaded with a coaxial dielectric rod, $\varepsilon(r)$ and $k_\perp$ are the piecewise constant functions, which equal $\varepsilon_1 = \varepsilon_r\left(1 + i\tan\delta\right)$ and k_1 for $0 \le r < R_i$ and $\varepsilon_2 = 1$ and k_2 for $R_i < r < R$. In this case, $h_z(r)$ and $e_z(r)$ can be written as [37, 38]

$$h_z(r) = \begin{cases} A_1 J_m(k_2 r) + A_2 N_m(k_2 r), & R_i \le r < R \\ A_3 J_m(k_1 r), & 0 \le r \le R_i \end{cases} \qquad (4)$$
$$e_z(r) = \begin{cases} A_4 J_m(k_2 r) + A_5 N_m(k_2 r), & R_i \le r < R \\ A_6 J_m(k_1 r), & 0 \le r \le R_i \end{cases}$$

where $J_m(\cdot)$ and $N_m(\cdot)$ are the m-th order Bessel and Neumann functions, respectively, and $k_{1,2}^2 = \varepsilon_{1,2} k^2 - k_z^2$. The constants A_i ($i = 1, 2..., 6$) are determined by the boundary conditions on the conducting surface of the gyrotron cavity

$$e_\varphi(R) = Z_s h_z(R),\ e_z(R) = -Z_s h_\varphi(R) \qquad (5)$$

and the continuity conditions for $h_z(r)$, $e_z(r)$, $h_\varphi(r)$ and $e_\varphi(r)$ at the vacuum-dielectric interface $r = R_i$, where $Z_s = (1-i)kd/2$, $d = \sqrt{2/(\mu_0 \omega \sigma)}$ is the skin-depth, and σ is the wall conductivity. From these conditions one obtains the dispersion relation for normal modes of a metal gyrotron cavity loaded with a coaxial dielectric rod.

In the general case, the normal modes of a dielectric-loaded cavity are hybrid modes ($h_z \neq 0$, $e_z \neq 0$). The exceptions are axially-symmetric modes ($m = 0$) and cutoff modes ($k_z = 0$), which have pure TE ($e_z = 0$) and TM ($h_z = 0$) polarizations. These modes are described by simplified dispersion relations, which can also be used as a good

approximation for near-cutoff modes ($\left|k_z^2/k^2\right| << 1$). For near-cutoff (quasi-) TE modes ($\left|e_z/h_z\right| << 1$) of a metal cavity with a coaxial dielectric rod the simplified dispersion relation can be found in [13].

The general dispersion relation establishes the connection between the axial wavenumber k_z and complex eigenvalue $k_\perp R = \chi_{mn}\left(1 - i\left(1 - k_z^2 R^2/\chi_{mn}^2\right)/\left(2Q_{ohm}\right)\right)$ of a normal mode of the dielectric-loaded cavity. Here Q_{ohm} is the ohmic quality factor. Alternatively, Q_{ohm} can be found from the following expression [39]:

$$Q_{ohm}^{-1} = Q_s^{-1} + Q_\delta^{-1}, \tag{6}$$

$$Q_s^{-1} = p_s \operatorname{Re} Z_s = \operatorname{Re} Z_s \frac{\left|h_z(R)\right|^2 + \left|h_\varphi(R)\right|^2}{kR^{-1}\int_0^R rdr\left|\mathbf{h}(r)\right|^2},$$

$$Q_\delta^{-1} = p_\delta \tan\delta = \tan\delta \frac{\varepsilon_r \int_0^{R_i} rdr\left|\mathbf{e}(r)\right|^2}{\varepsilon_r \int_0^{R_i} rdr\left|\mathbf{e}(r)\right|^2 + \int_{R_i}^R rdr\left|\mathbf{e}(r)\right|^2}$$

where Q_s and Q_δ are the quality factors associated with ohmic losses in metal walls and dielectric loading, respectively. The ohmic Q-values found from the dispersion relation and equation (6) must be equal to ensure the power balance in a metal gyrotron cavity loaded with a coaxial dielectric insert.

In gyrotrons, of prime importance are near-cutoff TE modes. For $R = 1.593$ mm and $\sigma = 2.9\times10^7$ S/m, Fig. 1 shows cutoff frequencies and ohmic Q-values of the lowest-order normal $TE_{11,n}$ modes versus the radius $R_i = C_i R$ of the coaxial insert, which is supposed to be a CVD diamond rod with $\varepsilon_r = 5.63$ and $\tan\delta = 10^{-5}$ [24-27]. As discussed in [13], these modes can be roughly classified as vacuum and dielectric modes depending on the radial structure of the electromagnetic field. The normal modes are called vacuum or dielectric modes, if their fields are concentrated inside the vacuum or dielectric regions of the cavity, respectively. It is notable that the frequencies of vacuum and dielectric modes are determined by the radius R of the metal cavity and the radius R_i of the dielectric insert, respectively. According to such classification, pure vacuum and dielectric modes are only modes of a cylindrical metal cavity completely filled with vacuum ($C_i = 0$) and dielectric ($C_i = 1$), respectively. Despite this, dielectric-like modes can also be supported by a cavity with relatively small transverse dimensions of the dielectric insert. Examples are normal TE modes with cutoff frequencies indicated by the symbols **A**, **B**, and **C** in Fig. 1. The distribution of their fields in the transverse cross-section of the diamond-loaded gyrotron cavity is shown in Fig. 2. It can be seen that indeed these modes feature field concentration inside the dielectric loading. Assuming for the moment that a cavity mode has a vanishing field outside the dielectric insert, one obtains $p_s \to 0$ and $p_\delta \to 1$. For such an idealized mode, the wall losses in metal cavity reduce to zero ($Q_s \to \infty$) and the ohmic quality factor $Q_{ohm} = Q_\delta$ approaches the value of $1/\tan\delta$ (see (6)), no matter what the outer wall conductivity is. This gives an insight into why the dielectric modes **A**, **B**, and **C** are high-Q normal modes of the metal gyrotron cavity loaded with ultralow-loss CVD diamond rod (Fig. 1b). Note that such modes should not be confused with normal modes of a cylindrical dielectric fiber in free space, which can only support slow waves ($k_z > k$) [37, 38, 40].

Although the fields of dielectric modes are mainly concentrated inside the dielectric, such modes can interact with a helical electron beam propagated through the vacuum region of a dielectric-loaded gyrotron cavity. To be efficient such beam-wave interaction requires the electron beam to be placed relatively close to the radius R_i of the coaxial dielectric insert [13, 41]. This can be seen from Fig. 3, which shows the coefficients of beam coupling with the second-harmonic dielectric modes **A**, **B**, and **C** versus the beam radius r_b. In this figure, the results for the pure vacuum second-harmonic $TE_{11,2}$ mode of a hollow gyrotron cavity ($C_i = 0$) are also depicted for comparison purpose. As evident from Fig. 3, the vacuum $TE_{11,2}$ mode and the dielectric mode **A** have identical beam-wave coupling coefficients for that beam radius, which ensures the strongest beam-wave coupling in the hollow gyrotron cavity. In other words, for the dielectric mode one can achieve the same strength of the beam-wave interaction as for the vacuum mode without change in design of the electron gun and metal gyrotron cavity. This suggests that high-Q dielectric modes introduced by ultralow-loss CVD diamond loading can be utilized as operating modes in gyrotrons. Examples of such a modification in gyrotron design are given in the subsequent Sections. In the following, we use the self-consistent single-mode code [23], which was updated to take into account the effect of a coaxial dielectric insert of the gyrotron cavity on the complex eigenvalue and beam-wave coupling coefficient of the operating near-cutoff TE mode [13]. In the single-mode approximation, the coupling between normal modes is assumed to be negligible and the field expansion (1) is thus replaced by a single non-vanishing term.

3. Output power of a gyrotron with diamond-loaded cavity

As an example, a cylindrical-cavity gyrotron with operating parameters, which are similar to those of the second-harmonic 527-GHz gyrotron developed in MIT, is considered [17]. The parameters of the electron beam are as follows: beam radius $r_b = 0.97$ mm, beam voltage $V_b = 16.7$ kV, pitch factor $\alpha = 1.85$, and beam current $I_b = 70$ mA. Velocity spread is neglected. The gyrotron operates in the $TE_{11,2,q}$ mode of a conventional three-section cylindrical cavity, where q is the axial mode index. The cavity is made from copper with the DC conductivity $\sigma = 2.9 \times 10^7$ S/m, which is one-half that for ideal OFHC copper. The main uniform section of the cavity has a radius of 1.593 mm and a length of 25 mm. The taper angles of the input and output sections equal $2°$ and $0.36°$, respectively. In the cold cavity, the diffractive Q_{dif} and ohmic Q_{ohm} quality factors of the operating mode are $97400/q^2$ and 7500, respectively. Thus, in this cavity, the operating mode can lose more than 90% of its power by heating of the cavity walls [17].

Such a drastic effect of ohmic wall losses on gyrotron operation can also be seen from Fig. 4a, which shows the calculated total $P_{tot} = \eta_{el} I_b V_b$ and output P_{out} power of the second-harmonic 527-GHz gyrotron versus the operating magnetic field B_0, where η_{el} is the interaction efficiency. It can be seen that the ratio P_{out}/P_{tot} of the output power to the total power indeed can be as small as 10% for this gyrotron. In addition, it should be stressed that the ohmic wall losses do more than lower the ratio P_{out}/P_{tot}. These losses also reduce the efficiency η_{el} of beam-wave interaction, together with total power P_{tot}. Such a loss-induced effect is explained by the reduction of the beam-wave interaction strength and makes an additional contribution to the degradation of output power in gyrotrons [23]. As a result, for selected operating parameters, the peak output power of the second-harmonic 527-GHz gyrotron is a mere 15 W due to extremely high ohmic losses in the copper cavity.

As a way to reduce ohmic losses we first consider the design of a gyrotron operated in high-Q dielectric modes **A** and **B**. These modes are supported by the same copper cavity, which is additionally loaded with an ultralow-loss CVD diamond rod ($\varepsilon_r = 5.63$ and $\tan\delta = 10^{-5}$). For the modes **A** and **B** the radius of the diamond rod inside the main cavity section was set to 0.793 mm ($C_i = 0.498$) and 0.677 mm ($C_i = 0.425$), respectively. As a result, in this section, the modes **A** and **B** have identical ohmic Q-values of 91630 (Fig. 1b) and the cutoff frequencies of about 484.9 GHz and 568.3 GHz (Fig. 1a), respectively. For both modes the beam-wave coupling coefficients were kept the same as for the vacuum $TE_{11,2}$ mode of original hollow cavity. As Fig. 3 suggests, in the diamond-loaded cavity, the desired beam-wave coupling strength for the dielectric modes **A** and **B** can be attained using the design value of the beam radius $r_b = 0.97$ mm and the modified value $r_b = 0.82$ mm, respectively. At this point, it is assumed that the eigenvalue χ_{mn} of the operating dielectric mode remains constant along the gyrotron cavity. This eliminates the change of the diffractive cavity losses due to variation of χ_{mn} and can be achieved by proper tapering of the CVD diamond rod.

Fig. 4b shows the starting currents of the second-harmonic ($s = 2$) dielectric modes **A** and **B** and the vacuum $TE_{11,2}$ mode versus the resonance mismatch $\Delta = 2\beta_{\perp 0}^{-2}\left(1 - s\,\omega_{c0}/\omega\right)$ [42, 43], where $\beta_{\perp 0}^{-2} = \left(1+\alpha^{-2}\right)\Big/\left(1-\gamma^{-2}\right)$, $\gamma = 1 + eV_b\Big/\left(m_e c^2\right)$, $\omega_{c0} = eB_0\Big/\left(m_e c\gamma\right)$, e and m_e are the electron charge and rest mass, respectively. As was shown in [23], the ohmic losses lower the beam-wave interaction strength in a gyrotron cavity. Such loss-induced effect is self-consistent and is attributed to the decrease in hot quality factor $Q_{tot} = Q_{dif} Q_{ohm}\Big/\left(Q_{dif} + Q_{ohm}\right)$ of the cavity. It tends to increase the starting current of the operating mode and shifts its oscillation region to lower values of the resonance mismatch (higher values of the guiding magnetic field B_0). These findings of [23] are consistent with data depicted in Fig. 4b. As can be seen, the lowest starting current can be achieved for the dielectric mode **B**, which possesses the highest frequency and consequently the highest diffractive (and total) quality factor. For this mode, the minimum starting current is about 7 times lower than that of the vacuum $TE_{11,2}$ mode. This suggests the possibility to reduce the cavity length or to move the beam radius r_b farther away from the diamond insert, with the result that the starting current of the dielectric mode still remains sufficiently low. Such a possibility can facilitate optimization of the mechanical gyrotron design. At the same time, it should be kept in mind that the change of the beam radius will also affect the mode competition, which must be extensively investigated to get a complete gyrotron design. Such investigations, however, are beyond the scope of the present study.

For the operating high-Q modes **A** and **B** of the second-harmonic gyrotron with the diamond-loaded cavity, the total and output power versus B_0 are shown in Fig. 5. Compared to the vacuum $TE_{11,2}$ mode, these modes have much higher output power. To be specific, the peak output power of the gyrotron can be increased from 15 W to about 140 W by replacing the operating $TE_{11,2}$ mode with either the mode **A** or the mode **B**. Such a drastic increase in the gyrotron output power is caused by a rise in both the interaction efficiency η_{el} and the ratio P_{out}/P_{tot} of the output power to the total power.

The data obtained demonstrate the fascinating and unique feature of high-Q dielectric modes of a diamond-loaded gyrotron cavity. These data, however, result from the simplified theoretical description and therefore leaves some practical issues unresolved. Firstly, it was assumed that the diamond rod is tapered. In practice, such a rod is difficult if not impossible to fabricate. Secondly, no account was taken of the ends of the finite-length diamond rod. The left end of the rod can be mounted in a holder and must be located away to the left from cutoff narrowing of the input (left) cavity section. In this section, the field of the operating mode is vanishingly small and therefore one might expect only a slight effect of the left end of the coaxial diamond insert on gyrotron operation. By contrast, the right end of this insert should be located in the output (right) cavity section, in which the field amplitude of the operating mode differs noticeably from zero. In such a situation, the diamond-loaded gyrotron cavity must also serve as a cavity with mode transformation (conversion). In this cavity, the operating mode is required to be a weakly-attenuated dielectric mode, which is transformed to the outgoing vacuum mode in the output cavity section, where the dielectric insert is terminated. Obviously, the desired cavity with mode transformation should be carefully designed to avoid degradation of the gyrotron performance, including output power and mode purity. Such a design must rely on the approach, which takes into account the coupling between normal modes of a diamond-loaded cavity.

4. Diamond-loaded cavity for a 527-GHz gyrotron

The challenge now is to design a copper cavity loaded with coaxial diamond rod for a second-harmonic 527-GHz gyrotron. From the practical standpoint, the diamond rod is required to be uniform and to have as short length as possible. On the other hand, this rod must induce only a small conversion of the operating mode to unwanted (spurious) normal modes in order to produce only a minor adverse effect on the gyrotron operation.

The required design of a diamond-loaded gyrotron cavity can be done using the mode-matching technique in the cold cavity case (without electron beam). In essence, this technique can be applied in a similar way as for a non-uniform metal cavity [29, 44], dielectric-coated cavity [34], and metal cavity with distributed wall corrugations [35]. The cavity is modeled by stepwise functions $R = R(z)$ and $R_i = R_i(z)$ and thus is represented as a sequence of jointed uniform copper waveguides loaded with coaxial diamond rods. In each waveguide, the electromagnetic field is expanded in terms of normal modes (1).

The normal modes of two joined waveguides are coupled. Let the superscripts I and II denote the characteristics of the first and second waveguides, respectively, and the condition $R^{\mathrm{I}} \le R^{\mathrm{II}}$ holds true. In this case, the coefficients of mode coupling are given by [34, 35]

$$T_{nl} = \int_0^{R^{\mathrm{I}}} rdr \left\langle \mathbf{e}^{\mathrm{I}}_{\perp n}, \mathbf{h}^{\mathrm{II}}_{\perp l} \right\rangle \tag{7}$$

where the integral

$$\int rdr \left\langle \mathbf{e}^{\mathrm{I}}_{\perp}, \mathbf{h}^{\mathrm{II}}_{\perp} \right\rangle = ir \frac{k_z^{\mathrm{I}} \left(e_z^{\mathrm{I}} h_\varphi^{\mathrm{II}} - e_z^{\mathrm{II}} h_\varphi^{\mathrm{I}} \right) - k_z^{\mathrm{II}} \left(e_\varphi^{\mathrm{I}} h_z^{\mathrm{II}} - e_\varphi^{\mathrm{II}} h_z^{\mathrm{I}} \right) + \left(\varepsilon^{\mathrm{I}} - \varepsilon^{\mathrm{II}} \right) k e_r^{\mathrm{I}} e_z^{\mathrm{II}}}{\left(k_\perp^{\mathrm{I}} \right)^2 - \left(k_\perp^{\mathrm{II}} \right)^2} \tag{8}$$

can be used for each concentric region of the first and second waveguides, in which $\varepsilon^{\mathrm{I}}(r)$ and $\varepsilon^{\mathrm{II}}(r)$ are both constant.

The coupling coefficients T_{nl} relate the field amplitudes of normal modes at the junction between two diamond-loaded waveguides. Generally, these modes are hybrid modes and include far-from-cutoff modes. In line with the orthogonality condition (2), the mode coupling coefficients reduce to zero in the extreme case of $R^{\mathrm{I}} = R^{\mathrm{II}}$ and $R_i^{\mathrm{I}} = R_i^{\mathrm{II}}$ ($\varepsilon^{\mathrm{I}}(r) = \varepsilon^{\mathrm{II}}(r)$), provided that $k_z^{\mathrm{I}} \ne k_z^{\mathrm{II}}$. This is apparent when the boundary (2) and continuity conditions for the axial and azimuthal field components are considered in (7), (8). With the coupling coefficients (7) the cavity eigenfrequencies and eigenfields are found in the regular way from the continuity conditions for the transverse fields $\mathbf{E}_\perp$ and $\mathbf{H}_\perp$ at the junctions between jointed waveguides and the outgoing-wave boundary conditions at both ends of the open gyrotron cavity [29, 34, 35, 44].

The operating mode of the second-harmonic gyrotron was considered to be the dielectric mode with the eigenvalue of about 20.22, which corresponds to the radius ratio $C_i = 0.398$ for the main uniform section of the gyrotron cavity (see the blue curve in Fig. 1a). Thus to achieve the desired operating frequency of 527 GHz the radii of the main cavity section and uniform diamond rod were adjusted to 1.830 mm and 0.729 mm, respectively. The length of the main section was set to 20 mm to ensure relatively low starting current of the operating mode, together with high output power of the second-harmonic 527-GHz gyrotron. Then the dimensions of input and output cavity sections were optimized to fulfill the following requirements: vanishingly small leakage of the operating mode from the cavity input; high-purity transformation

of the operating dielectric mode to the outgoing vacuum $TE_{11,3}$ mode; small conversion of the operating mode to spurious modes; the shortest possible length of the diamond insert. Such a procedure resulted in the length of 10 mm, and taper angles of $3.5°$ and $2°$ for the input and output sections of the diamond-loaded cavity, respectively. It was considered that the output cavity end with the radius $R = 2.179$ mm and the radius ratio $C_i = 0.335$ is connected to an exit cylindrical waveguide of the same radius. In this waveguide, the coaxial diamond rod ends. The position of the rod end has a little effect on the characteristics of the gyrotron cavity, provided that the mode radiated from the cavity output has nearly the same transverse field structure as that of a pure vacuum mode supported by the empty part of the exit waveguide. This is the case for the present designed cavity loaded with coaxial diamond rod. Inside this cavity, the length of the diamond rod was considered to be equal to 40 mm.

The amplitudes of the coupled normal modes of the designed diamond-loaded cavity are shown in Fig. 6a, in which the same mode nomenclature is used as that for TE and TM modes of the exit waveguide. It is evident that the outgoing wave is almost the pure vacuum $TE_{11,3}$ mode as desired. Thus, it can be extracted from the gyrotron using a standard output system. The designed cavity features small leakage of the operating mode through the input end and operates as a cavity with mode transformation. This can be seen from Fig. 6b. The operating mode is the dielectric mode in the main section of the cavity and transforms to the vacuum $TE_{11,3}$ mode in the cavity output. The transformation process is accompanied by a rise of spurious modes with small amplitudes (Fig. 6a), which have a minor effect on characteristics of the diamond-loaded cavity.

In addition, Fig. 6a depicts the results of the single-mode approximation (SMA), which is commonly known as Vlasov approach [45]. SMA implies that $V_n(z)$ is the only nonzero amplitude in (1) and is governed by the one-dimensional wave equation (Helmholtz equation) for the operating near-cutoff TE mode with varying complex transverse wavenumber $k_\perp$. As Fig. 6a suggests, the results of SMA and mode-matching technique are in good agreement. This justifies the use of the self-consistent single-mode code for studying the beam-wave interaction in the designed diamond-loaded cavity of the 527-GHz gyrotron. By the same reasoning as before, the radius r_b of the electron beam in this cavity was set to 0.89 mm.

For the 527-GHz gyrotron equipped with the diamond-loaded cavity the starting current of the operating mode, the total and output power are shown in Fig. 7a. It can be seen that, owing to the low starting current, the gyrotron can operate in a relatively wide range of the guiding magnetic fields. In this range, the gyrotron output power exhibits the average value of 42 W and reaches a peak of 171 W, which is more than 11 times higher than that of original 527-GHz gyrotron with conventional cavity (Fig. 4a). The large power increase is attributed to ultralow-loss CVD diamond loading of the gyrotron cavity.

It is common knowledge that CVD diamond possesses exceptional thermal and mechanical properties, which make it suitable for application in high-power electronics [4, 46]. In addition, high-quality CVD diamonds exhibit extremely low loss tangents, which range from 5×10^{-6} to 5×10^{-5} for sub-terahertz frequencies [24-27]. Since the ohmic quality factors of the dielectric modes under consideration can be roughly estimated as $1/\tan\delta$ (Fig. 1b), this suggests that the use of a CVD diamond loading would be particularly advantageous for metal cavities with ohmic Q-values below 20000. An important point is also that CVD diamond can be lightly doped with nitrogen or boron to provide small electric conductivity [47], which only slightly affects the dielectric properties of a bulky diamond. This conductivity might be necessary to prevent a coaxial diamond rod of a gyrotron cavity from dielectric charging by beam electrons [48]. The desired rod can be fabricated by laser cutting from a CVD diamond disk or its broken fragment. At present, such discs can be grown with the diameter up to 180 mm and the thickness of about 2 mm [49].

An important practical issue is the robustness of the gyrotron performance against errors in cavity manufacturing. As mentioned above, the frequency of the operating dielectric mode is mainly determined by the radius R_i of the CVD diamond rod (see Fig. 1a), so that $k_1 R_i \approx \sqrt{\varepsilon_r}\, k R_i$ is nearly constant. This condition gives the estimation formula for the frequency shift $\delta f = -f\left(\delta R_i / R_i + 0.5\,\delta\varepsilon_r/\varepsilon_r\right)$ caused by a deviation δR_i of the rod radius and an uncertainty $\delta\varepsilon_r/\varepsilon_r$ in the permittivity measurement of the CVD diamond, where f, R_i and ε_r are the design values of the operating frequency, rod radius and permittivity, respectively. From this formula, the operating frequency of the gyrotron equipped with the designed diamond-loaded cavity can be estimated as 527 ± 1 GHz for the errors $|\delta R_i| = 1.5$ μm or $|\delta\varepsilon_r|/\varepsilon_r = 0.4$ %. These errors tend to shift the operating magnetic field from the design value and slightly change the gyrotron output power. It is expected that, in practice, an additional factor affecting the beam-wave interaction in the diamond-loaded cavity will be the misalignment of the diamond rod. This factor still needs to be explored in order to estimate acceptable gap between idealized and actual experimental conditions.

The distinguishing feature of operating dielectric modes is a small sensitivity to the cavity radius. This feature is seen in Fig. 7b and may favor further the development of miniaturized cavities for terahertz gyrotrons. Noteworthy also is that the attenuation of dielectric modes is only slightly affected by the conductivity of the cavity walls. This suggests the possibility to use lossy conducting materials (e.g. stainless steel) in diamond-loaded cavities for suppression of vacuum

competing modes by ohmic wall losses. Such mode discrimination in diamond-loaded cavities calls for further investigation.

5. Conclusions

The propagation characteristics have been investigated for dielectric modes of a metal gyrotron cavity, which is loaded with a coaxial rod made of ultralow-loss CVD diamond. It has been shown that these modes feature high ohmic quality factors and rather strong coupling with helical electron beams of conventional magnetron injection guns. Owing to these properties, the dielectric modes of a diamond-loaded cavity can serve as high-Q operating modes in terahertz gyrotrons. In the sub-terahertz-to-terahertz range, the ohmic losses are often very high for currently available gyrotrons with conventional copper cavities. The concrete example is the frequency-tunable second-harmonic 527-GHz gyrotron developed at MIT. In this gyrotron, the operating mode loses up to 93% of its power by ohmic heating of the cavity wall. To eliminate high ohmic losses it has been proposed to equip the existing copper cavity of the 527-GHz gyrotron with a coaxial diamond insert. Two modifications of such an insert have been considered to enable gyrotron operation in high-Q dielectric modes with frequencies of about 485 GHz and 586 GHz. In the former case, parameters of the original electron gun have been adopted. Both modifications have been shown to provide a large increase in gyrotron output power from 15 W to about 140 W. For a gyrotron operated at 527 GHz a new copper cavity loaded with a coaxial diamond rod has been designed using the mode-matching technique. The designed cavity has been optimized to ensure high-purity transformation of the operating high-Q dielectric mode to outgoing vacuum mode. It has been proven that the new diamond-loaded cavity enables more than 11-fold increase in the output power of the 527-GHz gyrotron. In addition, it has been found that the operation of this gyrotron is only slightly sensitive to errors in machining of the copper cavity, but can be affected by uncertainties in radius and permittivity of the CVD diamond rod.

Acknowledgement

The work of Vitalii I. Shcherbinin was supported by the Georg Forster Research Fellowship for Experienced Researchers from the Alexander von Humboldt Foundation.

References

1. R. J. Temkin, Int. J. Terahertz Sci. Technol. (2014) https://doi.org/10.11906/TST.001-009.2014.03.01
2. M. Y. Glyavin, T. Idehara, S. P. Sabchevski, IEEE Trans. Terahertz Sci. Technol. (2015) https://doi.org/10.1109/TTHZ.2015.2442836
3. M. Blank, P. Borchard, S. Cauffman, K. Felch, M. Rosay, L. Tometich, Int. J. Terahertz Sci. Technol. (2016) https://doi.org/10.11906/TST.177-186.2016.12.17
4. M. Thumm, J. Infrared Millim. Terahertz Waves (2020) https://doi.org/10.1007/s10762-019-00631-y
5. S. H. Kao, C. C. Chiu, K. F. Pao, K. R. Chu, Phys. Rev. Lett. (2011) https://doi.org/10.1103/PhysRevLett.107.135101
6. T. Saito, Y. Tatematsu, Y. Yamaguchi, S. Ikeuchi, S. Ogasawara, N. Yamada, R. Ikeda, I. Ogawa, T. Idehara, Phys. Rev. Lett. (2012) https://doi.org/10.1103/PhysRevLett.109.155001
7. N. S. Ginzburg, M. Y. Glyavin, A. M. Malkin, V. N. Manuilov, R. M. Rozental, A. S. Sedov, A. S. Sergeev, V. Y. Zaslavsky, I. V. Zotova, T. Idehara, IEEE Trans. Plasma Sci. (2016) https://doi.org/10.1109/TPS.2016.2585307
8. Q. Zhao, S. Yu, T. Zhang, IEEE Trans. Electron Devices (2017) https://doi.org/10.1109/TED.2017.2756635
9. V. I. Shcherbinin, V. I. Tkachenko, K. A. Avramidis, J. Jelonnek, IEEE Trans. Electron Devices (2019) https://doi.org/10.1109/TED.2019.2944647
10. T. I. Tkachova, V. I. Shcherbinin, V. I. Tkachenko, J. Infrared Millim. Terahertz Waves (2019) https://doi.org/10.1007/s10762-019-00623-y
11. V. I. Shcherbinin, Y. K. Moskvitina, K. A. Avramidis, J. Jelonnek, IEEE Trans. Electron Devices (2020) https://doi.org/10.1109/TED.2020.2996179
12. I. V. Bandurkin, A. P. Fokin, M. Y. Glyavin, A. G. Luchinin, I. V. Osharin, A. V. Savilov, IEEE Electron Device Lett. (2020) https://doi.org/10.1109/LED.2020.3010445
13. V. I. Shcherbinin, K. A. Avramidis, M. Thumm, J. Jelonnek, J. Infrared Millim. Terahertz Waves (2021) https://doi.org/10.1007/s10762-020-00760-9
14. T. I. Tkachova, V. I. Shcherbinin, V. I. Tkachenko, Z. C. Ioannidis, M. Thumm, J. Jelonnek, J. Infrared Millim. Terahertz Waves (2021) https://doi.org/10.1007/s10762-021-00772-z
15. V. I. Shcherbinin, IEEE Trans. Electron Devices (2021) https://doi.org/10.1109/TED.2021.3090348
16. A. C. Torrezan, S. T. Han, I. Mastovsky, M. A. Shapiro, J. R. Sirigiri, R. J. Temkin, A. B. Barnes, R. G. Griffin, IEEE Trans. Plasma Sci. (2010) https://doi.org/10.1109/TPS.2010.2046617
17. S. K. Jawla, R. G. Griffin, I. A. Mastovsky, M. A. Shapiro, R. J. Temkin, IEEE Trans. Electron Devices (2020) https://doi.org/10.1109/TED.2019.2953658
18. La Agusu, T. Idehara, H. Mori, T. Saito, I. Ogawa, S. Mitsudo, Int. J Infrared Millim. Waves (2007) https://doi.org/10.1007/s10762-007-9215-y
19. V. I. Shcherbinin, T. I. Tkachova, V. I. Tkachenko, IEEE Trans. Electron Devices (2018) https://doi.org/10.1109/TED.2017.2769219
20. Y. J. Huang, L. H. Yeh, K. R. Chu, Phys. Plasmas (2014) https://doi.org/10.1063/1.4900415

21. G. G. Denisov, M. V. Morozkin, A. P. Fokin, A. V. Chirkov, A. N. Kuftin, S. Yu. Kornishin, E. M. Tai, A. S. Sedov, M. D. Proyavin, A. I. Tsvetkov, M. Yu. Glyavin, Proc. IRMMW-THz (2019) https://doi.org/10.1109/IRMMW-THz.2019.8874359
22. M. Yu. Glyavin, A. V. Chirkov, G. G. Denisov, A. P. Fokin, V. V. Kholoptsev, A. N. Kuftin, A. G. Luchinin, G. Yu. Golubyatnikov, V. I. Malygin, M. V. Morozkin, V. N. Manuilov, M. D. Proyavin, A. S. Sedov, E. V. Sokolov, E. M. Tai, A. I. Tsvetkov, V. E. Zapevalov, Rev. Sci. Instrum. (2015) https://doi.org/10.1063/1.4921322
23. V. I. Shcherbinin, A. V. Hlushchenko, A. V. Maksimenko, V. I. Tkachenko, IEEE Trans. Electron Devices (2017) https://doi.org/10.1109/TED.2017.2730252
24. M. Thumm, Int. J. Infrared Millim. Waves (1998) https://doi.org/10.1023/A:1022514528711
25. R. Heidinger, G. Dammertz, A. Meier, M. K. Thumm, IEEE Trans. Plasma Sci. (2002) https://doi.org/10.1109/TPS.2002.1158309
26. V. V. Parshin, V. N. Derkach, B. M. Garin, R. Heidinger, J. Molla, V. G. Ralchenko, S.I. Tarapov, I. Danilov, S. E. Myasnikova, V. I. Polyakov, A. I. Rukovishnikov, Proc. IRMMW-THz (2005) https://doi.org/10.1109/ICIMW.2005.1572387
27. V. V. Parshin, M. Y. Tretyakov, M. A. Koshelev, E. A. Serov, IEEE Sensors J. (2013) https://doi.org/10.1109/JSEN.2012.2215315
28. A. W. Fliflet, M. E. Read, Int. J. Electron. (1981) https://doi.org/10.1080/00207218108901350
29. J. M. Neilson, P. E. Latham, M. Caplan, W. G. Lawson, IEEE Trans. Microw. Theory Techn. (1989) https://doi.org/10.1109/22.31074
30. M. Botton, T. M. Antonsen, B. Levush, K. T. Nguyen, A. N. Vlasov, IEEE Trans. Plasma Sci. (1998) https://doi.org/10.1109/27.700860
31. A. V. Maksimenko, V. I. Shcherbinin, A. V. Hlushchenko, V. I. Tkachenko, K. A. Avramidis, J. Jelonnek, IEEE Trans. Electron Devices (2019) https://doi.org/10.1109/TED.2019.2893888
32. A. V. Maksimenko, V. I. Shcherbinin, V. I. Tkachenko, J. Infrared Millim. Terahertz Waves (2019) https://doi.org/10.1007/s10762-019-00589-x
33. S. Y. Park, J. L. Hirshfield, Phys. Rev. E (2000) https://doi.org/10.1103/PhysRevE.62.1266
34. V. I. Shcherbinin, G. I. Zaginaylov, V. I. Tkachenko, "Cavity with distributed dielectric coating for subterahertz second-harmonic gyrotron," Problems Atomic Sci. Technol. 6 (106), 255 (2016).
35. V. I. Shcherbinin, V. I. Tkachenko, J. Infrared Millim. Terahertz Waves (2017) https://doi.org/10.1007/s10762-017-0386-x
36. J. G. Dil, H. Blok, Opto-Electron. (1973) https://doi.org/10.1007/BF01418077
37. C. Yeh, F. I. Shimabukuro, The Essence of Dielectric Waveguides, (Springer US, New York, 2008), pp. 136–167.
38. V. I. Shcherbinin, G. I. Zaginaylov, V. I. Tkachenko, Prog. Electromagn. Res. M (2017) https://doi.org/10.2528/PIERM16110902
39. J. Krupka, M. E. Tobar, J. G. Hartnett, D. Cros, J. M. L. Floch, IEEE Trans. Microw. Theory Techn. (2005) https://doi.org/10.1109/TMTT.2004.840572
40. E. Snitzer, J. Opt. Soc. Amer. (1961) https://doi.org/10.1364/JOSA.51.000491
41. D. B. McDermott, D. S. Furuno, N. C. Luhmann, Int. J Infrared Millim. Waves (1983) https://doi.org/10.1007/BF01009701
42. V. L. Bratman, M. A Moiseev, M. I. Petelin, R. É. Érm, Radiophys. Quantum Electron. (1973) https://doi.org/10.1007/BF01030898
43. V. A. Flyagin, A. V. Gaponov, M. I. Petelin, V. K. Yulpatov, IEEE Trans. Microwave Theory Tech. (1977) https://doi.org/10.1109/TMTT.1977.1129149
44. Wagner, G. Gantenbein, W. Kasparek, M. Thumm, Int. J. Infrared Millim. Waves (1995) https://doi.org/10.1007/BF02274811
45. S. N. Vlasov, G. M. Zhislin, I. M. Orlova, M. I. Petelin, G. G. Rogacheva, Radiophys. Quantum Electron. (1969) https://doi.org/10.1007/BF01031202
46. R. S. Balmer, J. R. Brandon, S. L. Clewes, H. K. Dhillon, J. M. Dodson, I. Friel, P. N. Inglis, T. D. Madgwick, M. L. Markham, T. P. Mollart, N. Perkins, G. A. Scarsbrook, D. J. Twitchen, A. J. Whitehead, J. J. Wilman, S. M. Woollard, J. Phys.-Condensed Matter (2009) https://doi.org/10.1088/0953-8984/21/36/364221
47. N. Yang, S. Yu, J. V. Macpherson, Y. Einaga, H. Zhao, G. Zhao, G. W. Swain, X. Jiang, Chem. Soc. Rev. (2019) https://doi.org/10.1039/C7CS00757D
48. J. P. Calame, A. M. Cook, IEEE Trans. Plasma Sci. (2017) https://doi.org/10.1109/TPS.2017.2748043
49. G. Aiello, S. Schreck, K. A. Avramidis, T. Franke, G. Gantenbein, J. Jelonnek, A. Meier, T. Scherer, D. Strauss, M. Thumm, M.Q. Tran, C. Wild, E. Woerner, Fusion Eng. Des. (2020) https://doi.org/10.1016/j.fusengdes.2020.111818

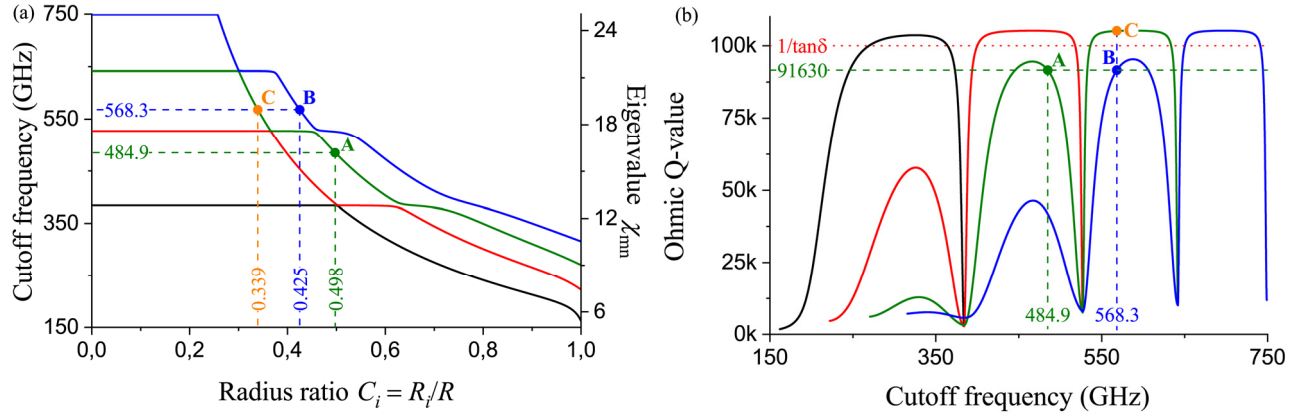

Fig. 1. (a) Cutoff frequencies, eigenvalues and (b) ohmic Q-values of the lowest-order normal $TE_{11,n}$ modes of the cylindrical copper cavity loaded with coaxial diamond rod ($R = 1.593$ mm, $n = 1, 2, 3, 4$).

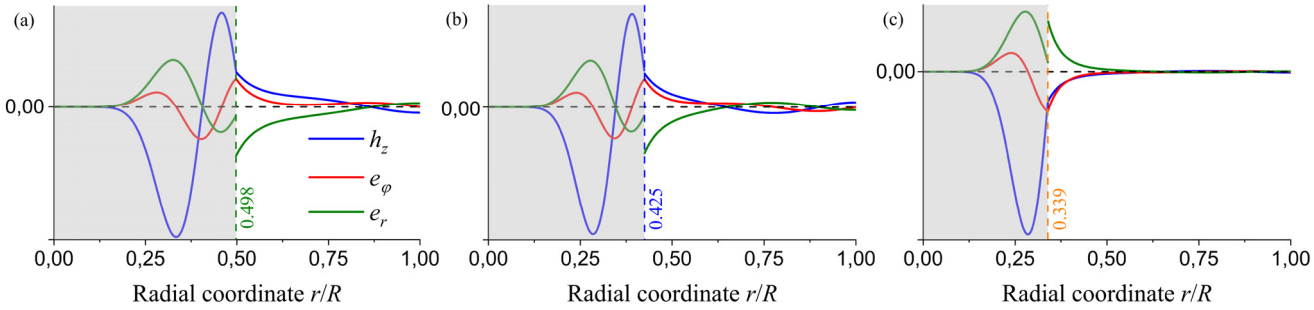

Fig. 2. Radial field structure for the dielectric modes (a) **A**, (b) **B** and (c) **C** with complex eigenvalues shown in Fig. 1.

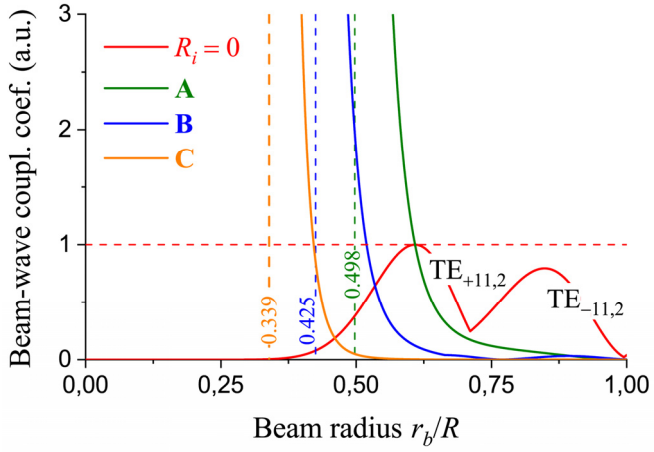

Fig. 3. Normalized beam-wave coupling coefficients versus the beam radius for the second-harmonic vacuum $TE_{\pm 11,2}$ modes and the dielectric modes **A**, **B** and **C**.

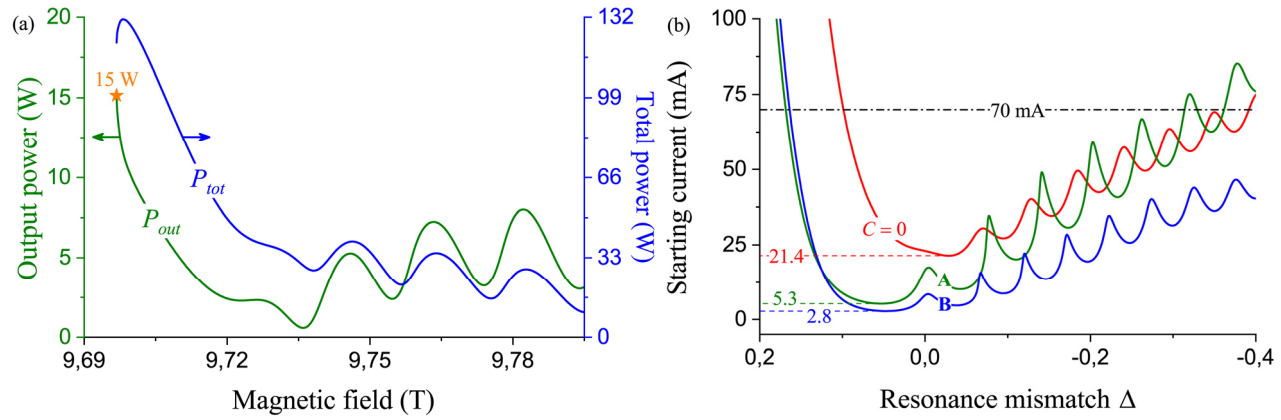

Fig. 4. (a) Total and output power of the conventional-cavity second-harmonic 527-GHz gyrotron developed at MIT and (b) starting currents for operating modes of the MIT gyrotron equipped with conventional and diamond-loaded cavities.

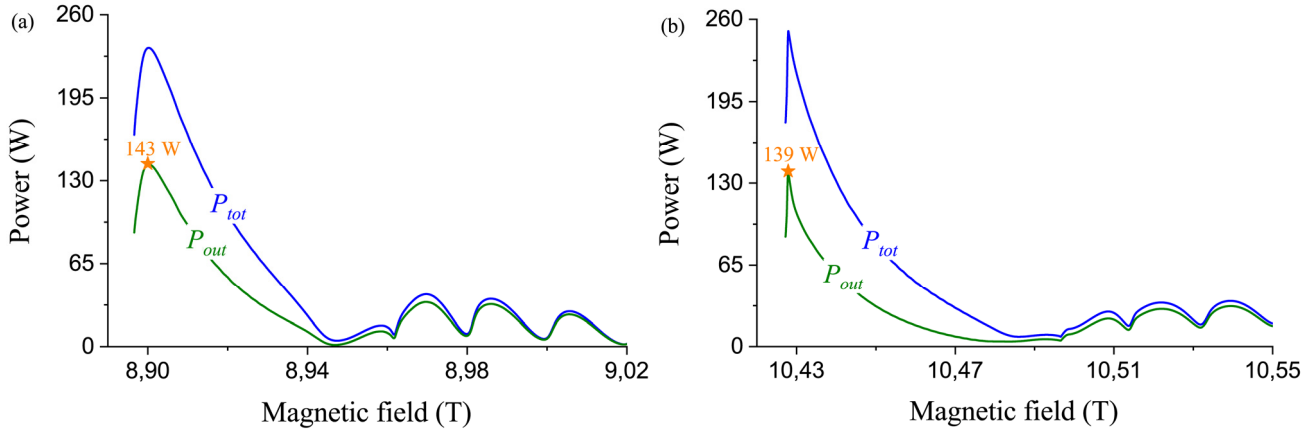

Fig. 5. Total and output power of the MIT gyrotron operated in high-Q dielectric modes (a) **A** and (b) **B** of the diamond-loaded cavity.

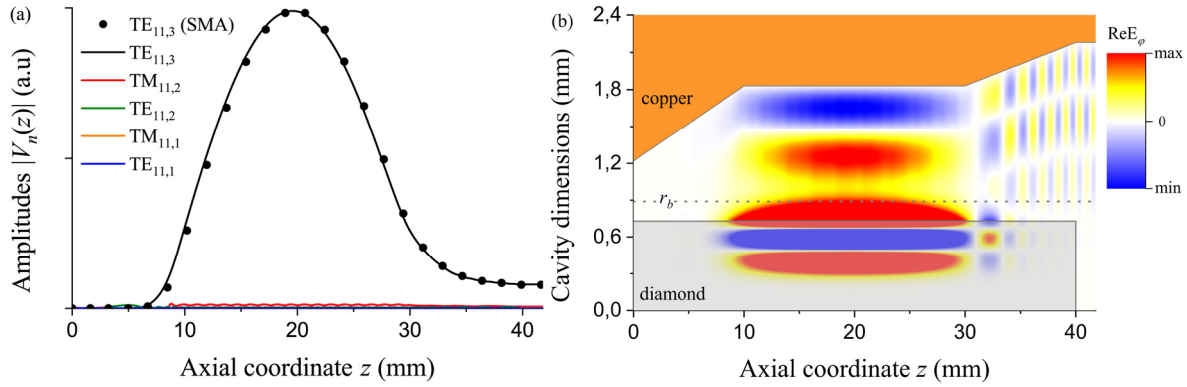

Fig. 6. (a) Amplitudes of normal modes and (b) field distribution for designed diamond-loaded cavity of the second-harmonic 527-GHz gyrotron.

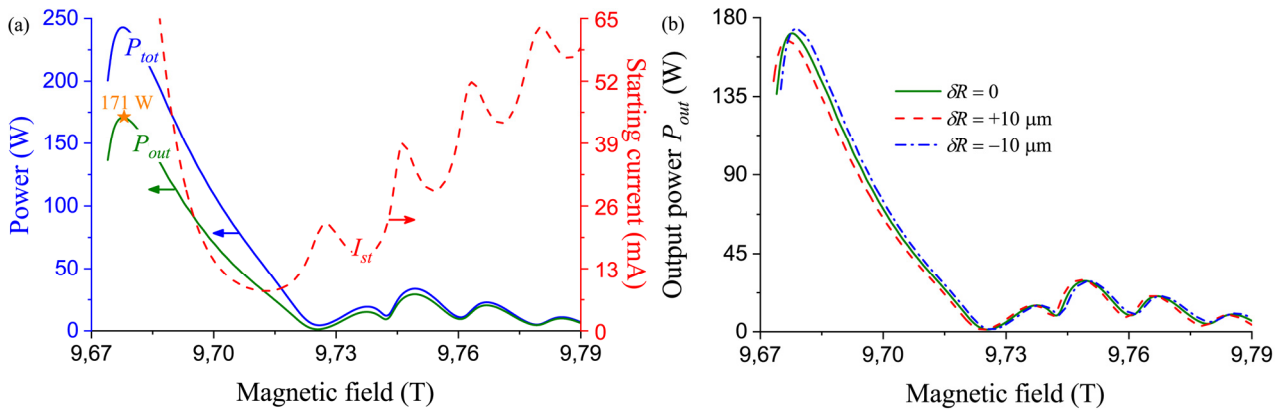

Fig. 7. (a) Starting current, total and output power of the high-Q operating mode of the 527-GHz gyrotron equipped with diamond-loaded copper cavity and (b) sensitivity of gyrotron operation to errors in machining of the copper cavity.